

Aberrantly expressed lncRNAs and mRNAs after botulinum toxin type A inhibiting salivary secretion

Qian-Ying Mao¹ | Shang Xie¹ | Li-Ling Wu² | Ruo-Lan Xiang²  | Zhi-Gang Cai¹

¹Department of Oral and Maxillofacial Surgery, Peking University School and Hospital of Stomatology, National Engineering Laboratory for Digital and Material Technology of Stomatology, Beijing, China

²Department of Physiology and Pathophysiology, Peking University School of Basic Medical Sciences, Key Laboratory of Molecular Cardiovascular Sciences, Ministry of Education, Beijing, China

Correspondence

Ruo-Lan Xiang, Department of Physiology and Pathophysiology, Peking University School of Basic Medical Sciences, No. 38 Xueyuan Road, Haidian District, Beijing, 100191, China.
Email: xiangrl@bjmu.edu.cn

Zhi-Gang Cai, Department of Oral and Maxillofacial Surgery, School and Hospital of Stomatology, Peking University, No. 22 Zhong Guan Cun South Street, Haidian District, Beijing, 100081, China.
Email: c2013xs@163.com

Funding information

This article was supported by the National Natural Science Foundation of China (Grant/Award Number: 81671007) and the Beijing Natural Science Foundation (Grant/Award Number: 7202078).

Abstract

Objective: In this study, we sought to determine the expression profiles of long non-coding RNAs (lncRNAs) and messenger RNAs (mRNAs) and construct functional networks to analyze their potential roles following botulinum toxin type A (BTXA)-mediated inhibition of salivary secretion.

Methods: The submandibular gland of rats in the BTXA and control groups was injected with BTXA and saline, respectively. Microarray analysis was used to identify the differentially expressed lncRNAs and mRNAs. Gene ontology and pathway analysis were performed to examine the biological functions. Functional networks, including lncRNA-mRNA co-expression and competing endogenous RNA (ceRNA) networks, were constructed to reveal the interaction between the coding and non-coding genes.

Results: Microarray analysis revealed that 254 lncRNAs and 631 mRNAs were differentially expressed between the BTXA and control groups. Bioinformatic analysis revealed that most of the mRNAs were closely related to transmembrane transporter activity. lncRNA-mRNA co-expression and ceRNA networks were constructed, and several critical mRNA-lncRNA axes and key microRNAs related to salivary secretion were identified.

Conclusions: Our study identified differentially expressed lncRNAs and mRNAs through microarray analysis and explored the interactions between the coding and non-coding genes through bioinformatic analysis. These findings provide new insights into the mechanism of BTXA-mediated inhibition of salivary secretion.

KEYWORDS

botulinum toxin type A, gene microarray analysis, lncRNA, mRNA, submandibular gland

1 | INTRODUCTION

Sialorrhea is a debilitating syndrome that manifests as the inability to control the continuous release of saliva, and is often associated with neurological disorders such as myasthenia gravis, amyotrophic lateral sclerosis, and Parkinson's disease (Srivanitchapoom, Pandey, & Hallett, 2014). Sialorrhea can lead to wet and foul clothes, chapped and irritated chin skin, reduced overall fluid and nutrition intake, and

in severe cases, suffocation, and aspiration pneumonia due to retention of saliva. Sialorrhea also exerts a negative impact on the physical and mental health of patients, who may experience social exclusion and isolation (Walshe, Smith, & Pennington, 2012). Therefore, it is necessary to find a safe and effective treatment for sialorrhea.

A few studies have shown that intraglandular injection of botulinum toxin type A (BTXA) is an effective treatment for sialorrhea (Vashishta, Nguyen, White, & Gillespie, 2013), but this method also



causes side effects such as dry mouth, difficulty in swallowing, and difficulty in opening and closing the mouth. It may even cause adverse reactions such as salivary duct stone, local injury of the carotid artery, or facial nerve branch (Naumann & Jost, 2004). However, the causes of these side effects remain unknown, which poses a challenge in clinical practice. Hence, it is necessary to understand the mechanism through which BTXA inhibits salivary secretion. Previous studies have suggested that BTXA mainly inhibits salivary secretion by the cleavage of synaptosomal-associated protein 25 and prevention of acetylcholine release (Wheeler & Smith, 2013). Our recent studies suggest that BTXA induces apoptosis of SMG-C6 cells (Shan, Xu, Cai, Wu, & Yu, 2013), AQP5 redistribution (Xu et al., 2015), and inhibits autophagic flux (Xie, Xu, Shan, & Cai, 2019). The mechanisms that cause these phenomena, however, remain unknown. Therefore, further studies are needed to understand the mechanism through which BTXA inhibits submandibular gland secretion. A better understanding of the underlying mechanism would contribute to more effective treatments for glandular hypersecretion diseases including sialorrhea.

Long non-coding RNAs (lncRNAs) are non-coding RNAs more than 200 nucleic acids in length. Studies have reported that lncRNAs are also closely associated with salivary gland diseases. For example, lncRNA ADAM metalloproteinase with thrombospondin type 1 motif 9 (ADAMTS9) antisense RNA 2 (ADAMTS9-AS2) promotes the migration and invasion of salivary adenoid cystic carcinoma by competitively binding to miR-143-3p (Xie et al., 2018). In human mucoepidermoid carcinoma, the abnormal fusion of CRTC1-MAML2 activates the downstream lncRNA, LINC00473, to regulate cell growth and survival (Chen et al., 2018). Analysis of the expression profile of the labial glands in patients with primary Sjögren's syndrome revealed 1,243 differentially expressed lncRNAs (Shi et al., 2016). In a recent study analysis of the expression profile of the submandibular gland in pleomorphic adenoma gene 1, transgenic mice revealed 9,110 differentially expressed lncRNAs (Xu et al., 2019). These differentially expressed lncRNAs may provide new insights into the pathogenesis of Sjögren's syndrome and pleomorphic adenoma, and may serve as potentially new therapeutic targets. Thus, lncRNAs are closely related to the occurrence, development, diagnosis, and treatment of salivary gland diseases.

A previous study reported that BTXA alters the expression profile of lncRNAs in human dermal fibroblasts (HDFS) and verified that BTXA downregulates the expression of FGFR3P in HDFS in a time-dependent manner, and upregulates the expression of FGFR3P and COL19A1 in a dose-dependent manner (Miao et al., 2017), suggesting that BTXA may play a role by altering the expression of lncRNAs. However, the effect of BTXA on the expression of lncRNA in the submandibular gland remains unclear. Therefore, first we generated an animal model in which BTXA inhibits the secretion of the submandibular gland, and then identified differentially expressed lncRNAs and mRNAs using microarray analysis following BTXA injection. Second, the functions of these RNAs were analyzed through Gene Ontology (GO) and Kyoto Encyclopedia of Genes and Genomes (KEGG) analysis. Finally, the lncRNA-mRNA co-expression

and competitive endogenous RNA (ceRNA) networks were constructed to predict the essential genes and interactions between the coding and non-coding genes.

2 | MATERIALS AND METHODS

2.1 | Experimental animals

Healthy adult male Sprague-Dawley rats (230–250 g) were purchased from the Laboratory Animal Service Center of the Peking University Health Science Center. All the rats were randomly divided into the control and BTXA groups. All the rats were anesthetized by intramuscular injection of ketamine (100 mg/kg body weight) and xylazine (5 mg/kg body weight). A median cervical incision was used to expose the submandibular glands. In the control group, the left gland was injected with 0.1 ml physiological saline, whereas in the BTXA group the left gland was injected with 6 U BTXA (Lanzhou Biochemical Co.) reconstituted in 0.1 ml physiological saline. Two weeks following the surgical procedure, the left glands were excised from all the rats and stored at -80°C immediately. All procedures were approved by the Ethics Committee for Animal Research, Peking University Health Science Center (approval number LA201494, 2014), and complied with the Guide for the Care and Use of Laboratory Animals (NIH Publication No. 85-23, revised 1996).

2.2 | Measurement of stimulated salivary flow from the submandibular gland

The rats were fasted for 5 hr. Following anesthesia, the submandibular duct was separated and inserted with a capillary tube under the microscope. The salivary flow was measured 5 min after intraperitoneal injection of pilocarpine (0.4 g/kg body weight) for 15 min.

2.3 | Histopathologic and immunohistochemical analyses

Submandibular gland tissues (5 μm) were fixed in 4% paraformaldehyde, incubated overnight at 4°C with hematoxylin and eosin (HE) or primary antibody to acetylcholinesterase (AChE; Servicebio), and then incubated with the secondary antibody conjugated with horseradish peroxidase at 37°C for 2 hr (Zhongshan Laboratories). ImageJ software (National Institutes of Health) was used for image analysis.

2.4 | Microarray analysis

The Arraystar Rat LncRNA V3.0 microarray (Arraystar) enables systematic profiling of rat lncRNAs along with the entire set of protein-coding transcripts and can detect approximately 10,333



lncRNAs and 28,287 protein-coding transcripts. Four samples were randomly selected from each of the control and BTXA groups. The RNA extraction was conducted using the TRIzol reagent (Invitrogen). The RNA quantity and quality were measured by NanoDrop ND 1000. The RNA integrity was assessed by standard denaturing agarose gel electrophoresis. The rRNA was removed from the total RNA to obtain the purified mRNA. Then, each sample was amplified and transcribed into fluorescent cRNA. The labeled cRNAs were purified using RNeasy Mini Kit (Qiagen) and then hybridized onto the microarray. The hybridized arrays were washed, fixed, and scanned using the Agilent DNA Microarray Scanner. Differentially expressed lncRNAs and mRNAs between the two groups were identified through fold change filtering and *p*-value (fold change >1.5, *p*-value < .05).

The microarray analysis was performed at KangChen Bio-tech. The microarray data have been deposited in the National Center for Biotechnology Information (NCBI) gene expression omnibus (GEO) database with the accession number GSE144985.

2.5 | GO and KEGG pathway analysis

GO mainly focuses on the biological functions of the differentially expressed mRNAs, including biological processes, molecular functions, and cellular components (*p*-value ≤ .05). The KEGG pathway analysis of differentially expressed transcripts was carried out using the KEGG database. *p*-values were calculated using Fisher's exact test, and the *p*-values were proofread using FDR value (*p*-value ≤ .05).

2.6 | Real-time quantitative reverse transcription-polymerase chain reaction (qRT-PCR)

Total RNA was isolated from the tissues using TRIzol reagent (Invitrogen) according to the manufacturer's instructions. The RevertAid First-Strand cDNA Synthesis Kit (Promega) was used to synthesize cDNA from 2 μg of RNA. The Thermo PikoReal PCR System (Thermo Fisher Scientific) was used for PCR. The reaction mix consisted of 5 μl DyNAmo Color Flash SYBR Green, 0.5 μl forward and reverse primers each, 2 μl cDNA, and 2 μl DEPC water in a total volume of 10 μl. GAPDH was used as the internal control, and the $2^{-\Delta\Delta C_t}$ method was used for analysis. The primers used for the lncRNAs and mRNAs are shown in Tables S1 and S2, respectively.

2.7 | Analysis of the lncRNA-mRNA co-expression network

Correlation network analysis was used to identify lncRNA-mRNA interactions. The ten validated lncRNAs were selected as the core genes to construct the co-expression network. After microarray

analysis, we obtained the normalized intensity of lncRNAs and mRNAs. The Pearson correlation coefficient between lncRNAs and mRNAs was calculated based on the normalized intensity. We chose the target genes to build the co-expression network by the Pearson correlation coefficient (absolute value) ≥ .9, *p*-value ≤ .05, and FDR ≤ 1.

2.8 | ceRNA network analysis

The validated lncRNAs were ultimately used to construct a ceRNA network, and the microRNAs (miRNAs) were predicted using miRanda and TargetScan. According to the principle that miRNA binds to the 3'UTR of mRNA and lncRNA, the target miRNAs were predicted using the R program. The ceRNA network was illustrated using Cytoscape (v2.8.3).

3 | RESULTS

3.1 | BTXA impaired the morphology and function of the submandibular gland

HE staining showed atrophy and irregular shape of the acinar cells in the BTXA group (Figure 1a). The area ratio of acini was decreased by 45% in each field of view in the BTXA group (Figure 1b). Immunohistochemical staining showed that the expression of AchE was decreased in the BTXA group (Figure 1c). AchE mainly degrades acetylcholine in the synaptic cleft, which indirectly suggests that BTXA prevented the release of acetylcholine. We also explored the effect of BTXA on the secretory function of the submandibular gland. In the BTXA group, the stimulated salivary flow rate was reduced by 70% (Figure 1d), and the stimulated salivary flow rate normalized to the gland weight was also decreased (Figure 1e). These results suggested that BTXA damaged the structure and secretory function of the submandibular gland. These results further demonstrated that the animal model was successfully constructed.

3.2 | Identification of differentially expressed lncRNAs and mRNAs

We used volcano plot and heat map to depict the differentially expressed lncRNAs and mRNAs in the control and BTXA groups. As shown in the volcano plot (Figure S1), 254 differentially expressed lncRNAs (123 upregulated and 131 downregulated) and 631 differentially expressed mRNAs (263 upregulated and 368 downregulated) were identified. The top 50 differentially expressed lncRNAs (Figure 2a) and mRNAs (Figure 2b) are depicted in the heat map. The top ten up- and downregulated lncRNAs and mRNAs with the largest fold changes are shown in Tables S3 and S4, respectively.

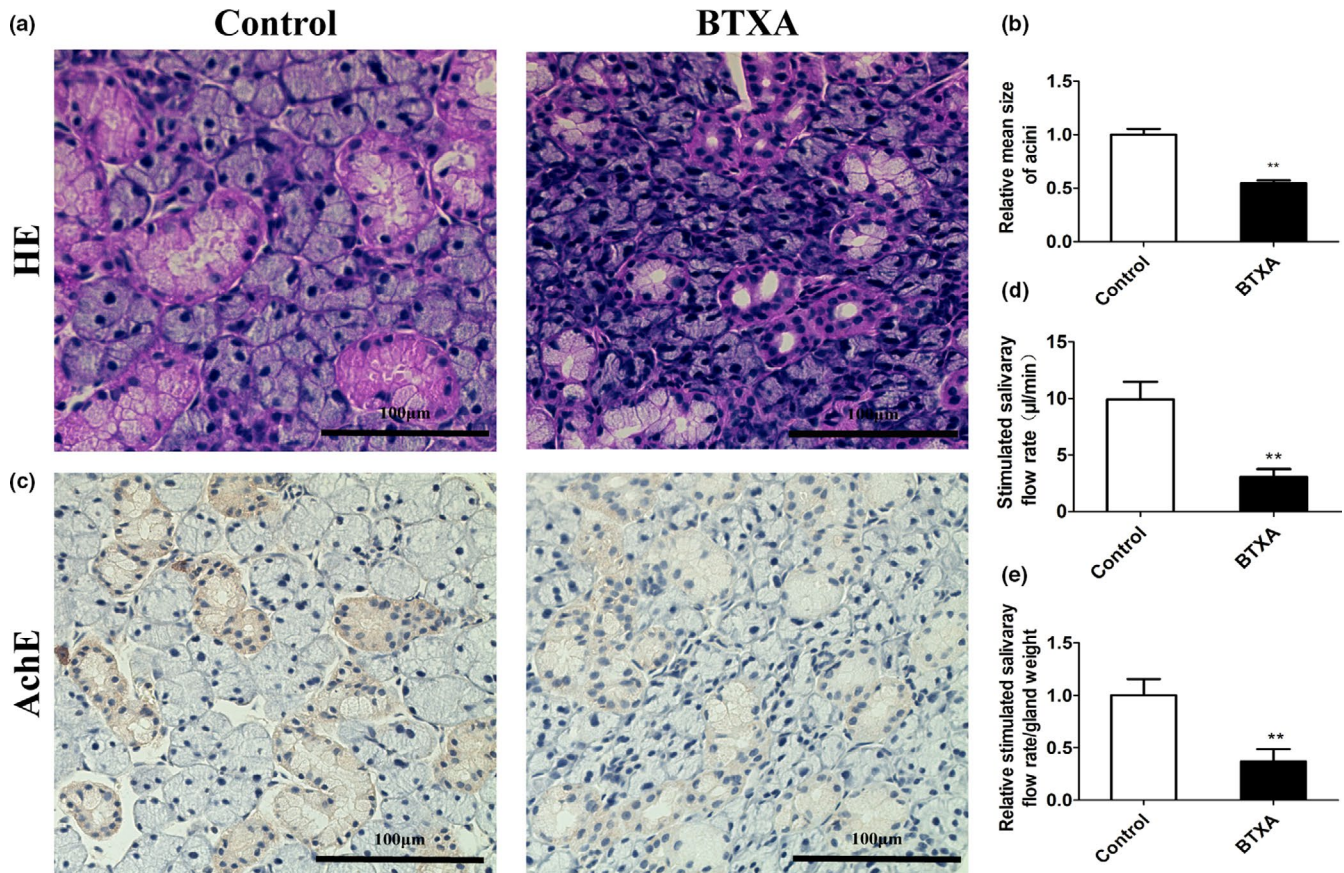


FIGURE 1 Morphology and secretion function were impaired after BTXA injection into submandibular gland of rats. (a) Hematoxylin and eosin (HE) staining of submandibular glands. Scale bars, 100 μm. (b) Relative mean size of acini cells. (c) Immunohistochemical staining of acetylcholinesterase of submandibular glands. Scale bars, 100 μm. (d) The stimulated salivary flow rate of submandibular glands (μl/min). (e) Relative normalized stimulated salivary flow rate by gland weight. $N = 5-7/\text{group}$, * $p < .05$, ** $p < .01$ [Colour figure can be viewed at wileyonlinelibrary.com]

3.3 | Validation of the expression levels of the differentially expressed lncRNAs and mRNAs

To confirm the results of the microarray analysis, several significant lncRNAs and mRNAs were validated using qRT-PCR. Following BTXA injection, the expression of AC094236.1, LOC103691854, LOC102546383, LOC103691771, and LOC102557384 was upregulated, whereas the expression of Fancm, AABR07053881.1, LOC103694955, AABR07065259.1, and uc.16 was downregulated (Figure 2c). These ten lncRNAs were selected for the subsequent construction of the network. Among the mRNAs that were verified, Ptgdr2, Fam220a, Rhbd11, and Fmo6 were upregulated, and Gys2, Cabp7, Ckap2, Ly6g6d, Kif20a, Spc24, and Dbp were downregulated following BTXA treatment (Figure 2d).

3.4 | GO and KEGG analysis

We performed GO and KEGG analysis of the differentially expressed mRNAs. The top ten GO terms related to biological processes, cellular components, and molecular functions of the up and downregulated mRNAs are shown in Figure S2. The top five GO terms are

shown in Table 1. Among them, inorganic molecular entity transmembrane transporter activity (GO: 0015318), monocarboxylic acid transmembrane transporter activity (GO: 0008028), transmembrane transporter activity (GO: 0022857), and cation transmembrane transporter activity (GO: 0008324) were highly enriched (Figure S2a). KEGG analysis of the upregulated mRNAs revealed that four pathways were significantly altered, among which C-type lectin receptor signaling pathway had the highest degree of enrichment (Figure S2c). Similarly, KEGG analysis of the downregulated mRNAs revealed that seven pathways were significantly altered, among which selenocompound metabolism ranked the highest (Figure S2d).

3.5 | Establishment of lncRNA-mRNA co-expression network

We constructed a lncRNA-mRNA co-expression network to explore the relationship between the lncRNAs and mRNAs following BTXA injection. The ten selected lncRNAs were used to predict the target genes among 631 differentially expressed mRNAs, and 397 mRNAs were thus obtained to construct a co-expression network (Figure 3). The results showed that LOC102546383 had the largest number of

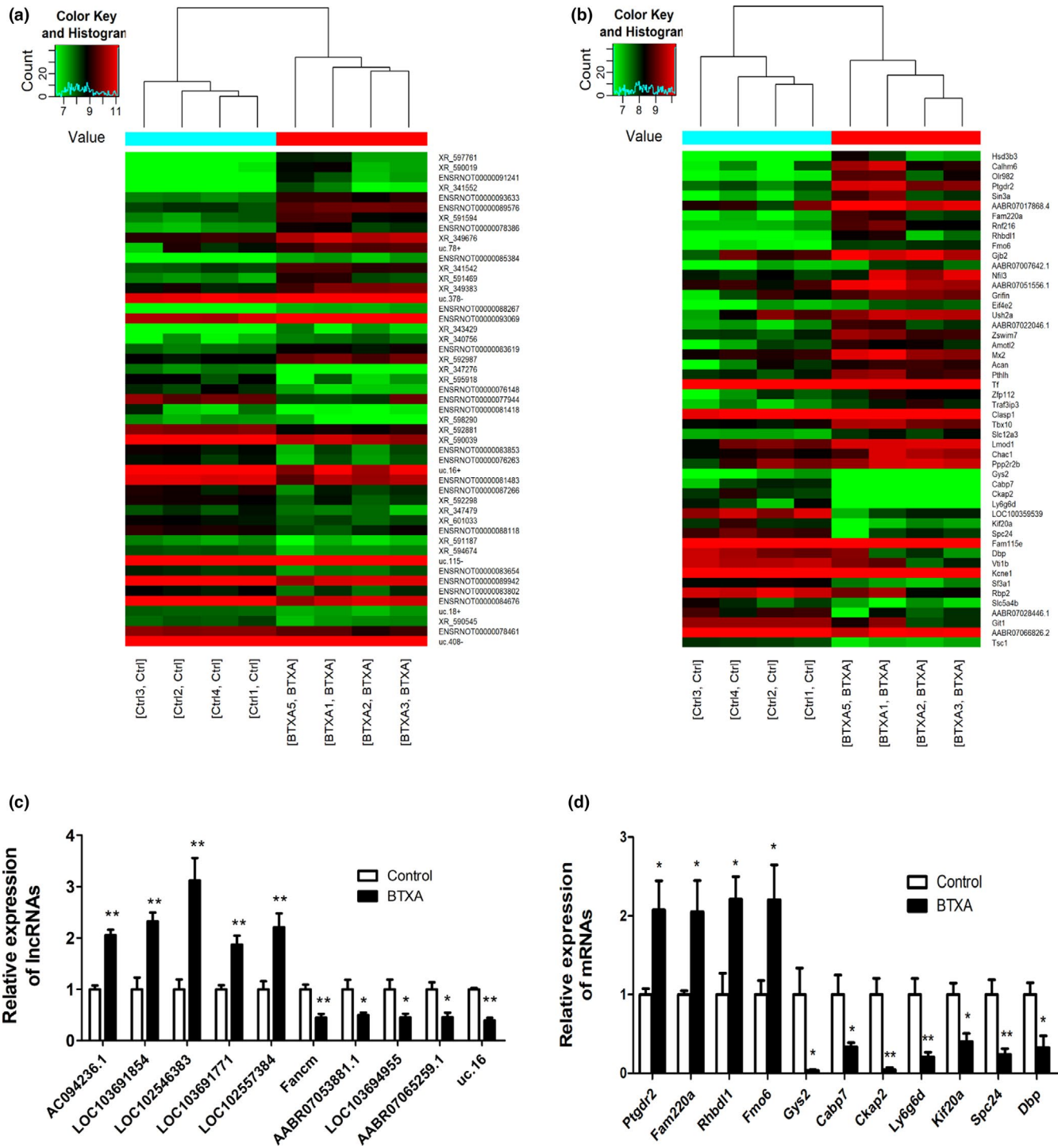


FIGURE 2 The expression microarray profiles of differentially expressed lncRNAs and mRNAs. The heat map was used to demonstrate the top 50 differentially expressed lncRNAs (a) and mRNAs (b). Validation of ten selected lncRNAs (c) and eleven selected mRNAs (d) by qRT-PCR. $N = 4/\text{group}$, $*p < .05$, $**p < .01$. Ptgdr2, prostaglandin D2 receptor 2; Fam220a, family with sequence similarity 220 member A; Rhbd1, rhomboid like 1; Fmo6, flavin-containing monooxygenase 6; Gys2, glycogen synthase 2; Cabp7, calcium-binding protein 7; Ckap2, cytoskeleton-associated protein 2; Ly6g6d, lymphocyte antigen 6 family member G6D; Kif20a, kinesin family member 20A; Spc24, SPC24 component of NDC80 kinetochore complex; Dbp, D-box binding PAR bZIP transcription factor [Colour figure can be viewed at wileyonlinelibrary.com]

target genes, 210 in total. The top ten positive and negative correlations are listed in Table 2. We used DAVID 6.8 database and found that the target gene aquaporin 5 (Aqp5) and transient receptor potential cation channel subfamily V member 6 (Trpv6) were related to

salivary secretion. The co-expression network showed that AQP5 was linked to three co-expressed lncRNAs (Fancm, LOC102546383, and AC094236.1). TRPV6 was linked to one co-expressed lncRNA (Fancm; see Table 3 for details).

TABLE 1 GO analysis of differentially expressed mRNAs

Regulation	Term	Domain	Count	p-value	Enrichment score
Up	Response to lead ion	Biological process	5	0.000205852	3.686445051
	Response to cobalt ion	Biological process	3	0.000820022	3.086174594
	Regulation of histone methylation	Biological process	5	0.001539436	2.812638406
	Regulation of cellular protein localization	Biological process	15	0.002239879	2.649775358
	Negative regulation of histone modification	Biological process	4	0.00248115	2.60534697
	Transcriptionally active chromatin	Cellular component	3	0.002331687	2.632329762
	Preribosome	Cellular component	5	0.003014062	2.520847791
	Small-subunit processome	Cellular component	3	0.010497112	1.978930165
	Plasma membrane-bounded cell projection	Cellular component	37	0.012538402	1.901757811
	Axon initial segment	Cellular component	2	0.012862193	1.890684982
	H4 histone acetyltransferase activity	Molecular function	3	0.00174045	2.759338348
	Inorganic molecular entity transmembrane transporter activity	Molecular function	20	0.00261805	2.582022049
	Monocarboxylic acid transmembrane transporter activity	Molecular function	4	0.003922273	2.406462129
	Transmembrane transporter activity	Molecular function	23	0.004631884	2.334242297
	Cation transmembrane transporter activity	Molecular function	16	0.005560524	2.254884274
Down	Cell division	Biological process	25	9.53133E-08	7.020846671
	Chromosome segregation	Biological process	20	2.13029E-07	6.671561948
	Nuclear chromosome segregation	Biological process	17	1.01973E-06	5.991513199
	Mitotic cytokinesis	Biological process	9	1.76678E-06	5.752817337
	Mitotic cell cycle process	Biological process	28	3.41822E-06	5.466200192
	Supramolecular polymer	Cellular component	33	3.01939E-06	5.520080503
	Supramolecular complex	Cellular component	33	3.0968E-06	5.509087092
	Cytoskeleton	Cellular component	57	4.58202E-06	5.338942608
	Microtubule cytoskeleton	Cellular component	39	6.92877E-06	5.15934399
	Supramolecular fiber	Cellular component	32	6.99396E-06	5.155276953
	Protein binding	Molecular function	152	5.32208E-05	4.273918935
	Tubulin binding	Molecular function	17	9.85506E-05	4.006340947
	Ion gated channel activity	Molecular function	15	0.000253069	3.596760229
	Cytoskeletal protein binding	Molecular function	30	0.000264518	3.577544068
	Gated channel activity	Molecular function	15	0.000279967	3.552892665

We also performed GO and KEGG analysis of the 397 mRNAs involved in the construction of the co-expression network (Figure S3). GO analysis revealed that chromosome segregation (GO: 0007059), supramolecular polymer (GO: 0099081), and inorganic molecular entity transmembrane transporter activity (GO: 0015318) were most significantly enriched in the biological process, cellular component, and molecular function domains, respectively. KEGG analysis suggested that porphyrin and chlorophyll metabolism pathways were most significantly enriched.

3.6 | Analysis of the ceRNA network

The Venn diagram (Figure 4a) shows the 147 target genes obtained from the intersection of 4,273 target genes of the ten selected

lncRNAs with the 631 differentially expressed mRNAs. The ten lncRNAs and 147 mRNAs were ultimately used to construct the ceRNA network (Figure 4b). As a result, 1,425 lncRNA-miRNA-mRNA pairs were obtained. We used the DAVID 6.8 database to perform functional analysis of the target genes and found that seven lncRNAs and nineteen mRNAs were related to salivary secretion (see Table 4 for details).

Meanwhile, we performed GO and KEGG of the 147 mRNAs involved in the construction of the ceRNA network (Figure S4). The results of the GO analysis indicated that cytoskeletal protein binding (GO: 0008092), plasma membrane-bounded cell projection (GO: 0120025), and cellular component organization (GO: 0016043) were highly enriched. KEGG analysis indicated that sulfur metabolism was the most enriched.

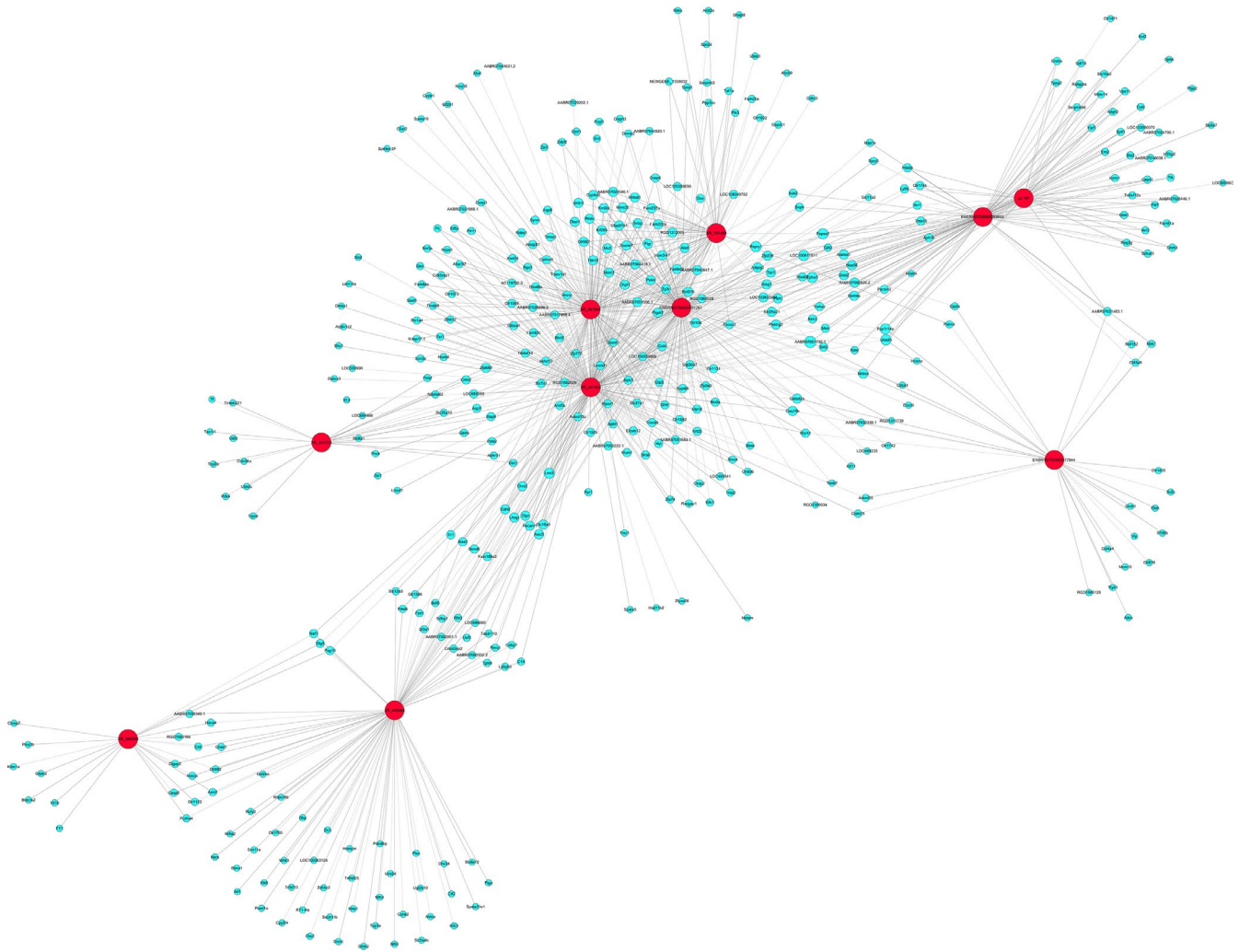


FIGURE 3 IncRNA-mRNA co-expression network analysis. Blue: lncRNA; red: mRNA; solid line: positive correlation; dotted line: negative correlation. ENSRNOT00000091241: AC094236.1; XR_591594: LOC103691854; XR_341542: LOC102546383; XR_591469: LOC103691771; XR_349383: LOC102557384; XR_347276: Fancm; ENSRNOT00000077944: AABR07053881.1; XR_598290: LOC103694955; ENSRNOT00000083853: AABR07065259.1; uc.16+: uc.16 [Colour figure can be viewed at wileyonlinelibrary.com]

4 | DISCUSSION

In this study, we successfully constructed an animal model of BTXA-mediated inhibition of submandibular gland secretion and obtained the expression profiles of lncRNAs and mRNAs through microarray analysis following BTXA injection. We found several significant differentially expressed lncRNAs and mRNAs and verified them using qRT-PCR (Figure 2c,d).

We further carried out functional annotation of the differentially expressed mRNAs through GO and KEGG pathway analyses. GO analysis of the upregulated mRNAs revealed that the biological functions were mainly related to the transmembrane transporter activity. Transmembrane transport plays an important role in salivary secretion. The transport of electrolytes across the epithelia results in fluid movement which is mediated by several membrane proteins on both apical and basolateral sides of epithelial cells (Ohana, 2015). $\text{Na}^+/\text{K}^+/\text{Cl}^-$ cotransporter (NKCC) mediates 70% of Cl^- ion transport into the acini and has an important

role in salivary secretion (Evans et al., 2000). Large conductance Ca^{2+} -activated K^+ channels and intermediate/small conductance Ca^{2+} -activated K^+ channels are imperative for stimulated secretion in parotid glands (Romanenko, Nakamoto, Srivastava, Melvin, & Begenisich, 2006). Solute carrier family 26 member 6 (Slc26a6) acts as both ion channels and Cl^- -dependent anion exchangers, mediating the migration of HCO_3^- and carboxylic acids (Ohana, Yang, Shcheynikov, & Muallem, 2009). Studies have shown that $\text{Cl}^-/\text{oxalate}$ exchange and $\text{Cl}^-/\text{HCO}_3^-$ exchange are markedly reduced in Slc26a6 $^{-/-}$ mice and oxalate secretion in saliva is also significantly reduced (Mukaibo et al., 2018). In conclusion, transmembrane transport plays a crucial role in regulating the composition and secretion of saliva. In our study, we found the following GO terms related to the transmembrane transport process: transmembrane transporter activity (GO: 0015318), monocarboxylic acid transmembrane transporter activity (GO: 0008028), transmembrane transporter activity (GO: 0022857), and cation transmembrane transporter activity (GO: 0008324). Among them, the



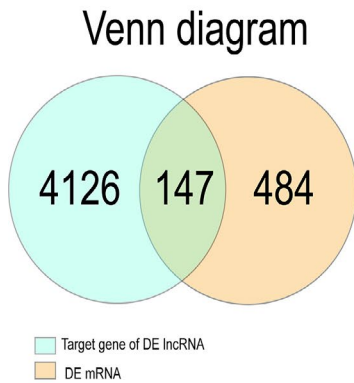
TABLE 2 The top 10 co-expression pairs

mRNA	Gene	lncRNA	Gene	Pcc	Pcc type	p-value
NM_012636	Pthlh	XR_591594	LOC103691854	0.996296	+	8.20E-10
ENSRNOT00000048829	AABR07051556.1	XR_591594	LOC103691854	0.99564	+	1.57E-09
ENSRNOT00000029692	Fam220a	XR_591594	LOC103691854	0.994093	+	5.29E-09
ENSRNOT000000033916	Naf1	XR_349383	LOC102557384	0.99342	+	8.14E-09
ENSRNOT000000054808	Ptgdr2	XR_341542	LOC102546383	0.992616	+	1.29E-08
ENSRNOT000000048455	Rabgta	uc.16+	uc.16	0.992539	+	1.34E-08
ENSRNOT000000003974	Zswim7	ENSRNOT000000091241	ENSRNOG00000058836	0.992253	+	1.56E-08
ENSRNOT000000054808	Ptgdr2	XR_591594	LOC103691854	0.991589007	+	1.35E-05
ENSRNOT000000059335	AABR07064415.1	ENSRNOT000000091241	AC094236.1	0.991543101	+	1.35E-05
ENSRNOT000000003974	Zswim7	XR_591594	LOC103691854	0.991115132	+	1.48E-05
ENSRNOT000000017562	Odf3	XR_347276	Fancm	0.99476777	-	3.26E-09
ENSRNOT000000088449	Pigr	ENSRNOT000000091241	ENSRNOG00000058836	-0.989945985	-	4.42E-08
ENSRNOT000000021254	Olr104	ENSRNOT000000091241	ENSRNOG00000058836	-0.986491506	-	1.43E-07
ENSRNOT000000089673	Arid5a	XR_341542	LOC102546383	-0.985058586	-	2.14E-07
ENSRNOT000000088449	Pigr	XR_341542	LOC102546383	-0.98497611	-	2.19E-07
ENSRNOT000000022481	Lhcgr	XR_341542	LOC102546383	-0.982323995	-	4.18E-07
ENSRNOT000000088449	Pigr	XR_591594	LOC103691854	-0.982093324	-	4.40E-07
ENSRNOT000000089022	Ripor1	ENSRNOT000000091241	ENSRNOG00000058836	-0.981179172	-	5.37E-07
ENSRNOT000000016401	Haus4	XR_349383	LOC102557384	-0.980496617	-	6.18E-07
ENSRNOT000000083125	Parn	XR_341542	LOC102546383	-0.9779611618	-	7.38E-07

TABLE 3 The co-expression pairs related to salivary secretion

mRNA	Gene	lncRNA	Gene	Pcc	Pcc type	p-value
ENSRNOT00000020616	Trpv6	XR_347276	Fancm	0.935778	+	6.88E-05
ENSRNOT00000084911	Aqp5	XR_347276	Fancm	0.917841	+	.00018
		XR_341542	LOC102546383	-0.91397	-	.001904
		ENSRNOT00000091241	AC094236.1	-0.95431	-	1.80E-05

(a)



(b)

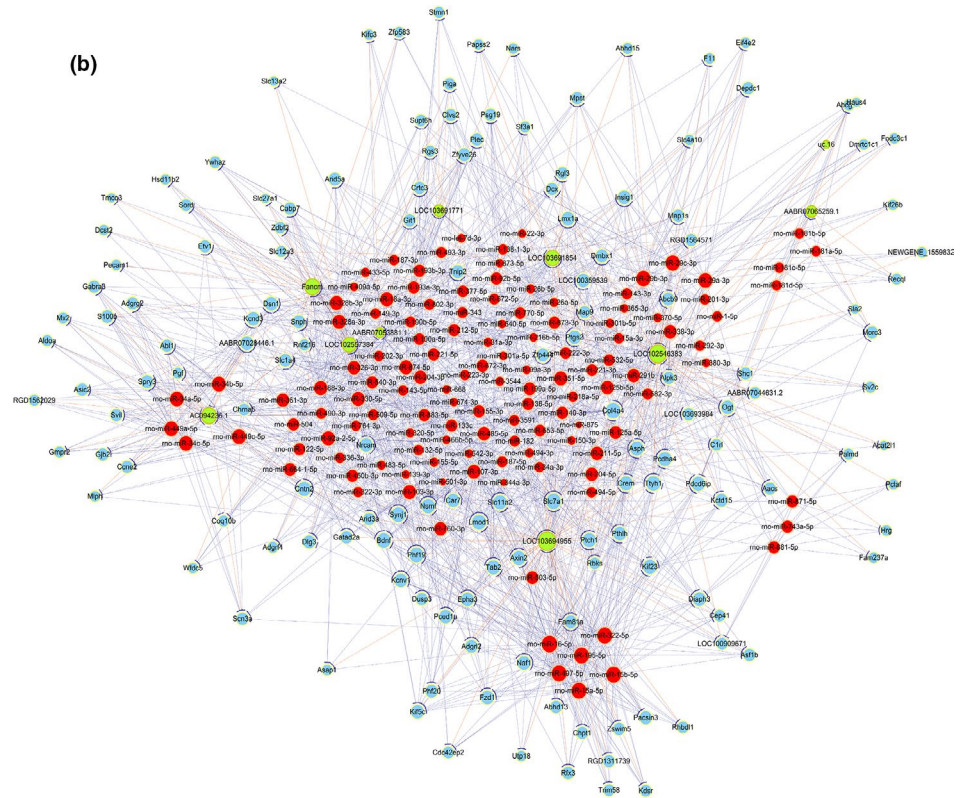


FIGURE 4 ceRNA network analysis. (a) Venn diagram and (b) ceRNA network between lncRNAs, mRNAs, and predicted miRNAs. Green: lncRNA; red: miRNA; blue: mRNA. ENSRNOT00000091241: AC094236.1; XR_591594: LOC103691854; XR_341542: LOC102546383; XR_591469: LOC103691771; XR_349383: LOC102557384; XR_347276: Fancm; ENSRNOT00000077944: AABR07053881.1; XR_598290: LOC103694955; ENSRNOT00000083853: AABR07065259.1; uc.16+: uc.16 [Colour figure can be viewed at wileyonlinelibrary.com]

inorganic molecular entity transmembrane transporter activity was highly enriched, suggesting that BTXA may affect the content of inorganic molecules in the saliva. However, it was reported that the differentially expressed mRNAs were enriched in positive regulation of collagen biosynthetic process (GO: 0032967) and positive regulation of fibroblast proliferation (GO: 0048147) after BTXA treatment of HDFS (Miao et al., 2017), showing the positive effects for remodeling skin. This difference identified that BTXA had various functions in treating different diseases. As for BTXA inhibition of salivary secretion, the changes in transmembrane transporter activity may play an important role.

We constructed co-expression and ceRNA networks of the validated lncRNAs and differentially expressed mRNAs to explore the interaction between the coding and non-coding genes. First, the co-expression network suggested that Fancm, LOC102546383, and AC094236.1 were involved in the regulation of Aqp5 expression.

Numerous studies have shown that the expression and distribution of Aqp5 are crucial for the regulation of salivary secretion (Delporte, 2014). Pilocarpine-stimulated salivary secretion decreased by 60% in Aqp5-knockout mice, and the saliva becomes viscous and hypertonic (Krane et al., 2001). The salivary secretion in Aqp5-knockout mice reduced, while the permeability of the paracellular barrier decreased significantly (Kawedia et al., 2007). Besides, salivary secretion is also affected by the distribution of Aqp5. For example, in the salivary glands of patients with Sjögren's syndrome, Aqp5 is mainly located in the basolateral membrane of the acinar cells (Steinfeld et al., 2001). In parotid gland (acini and ducts) of senescent rats, reduced translocation of Aqp5 to the apical membrane occurred during stimulated salivary secretion (Inoue, Iida, Yuan, Ishikawa, & Ishida, 2003). In our previous study, we also found that BTXA reduced the expression of Aqp5 in rabbits (Shan et al., 2013) and rats (Xu et al., 2015) and induced Aqp5 to translocate from the



TABLE 4 The ceRNA network related to salivary secretion

Gene symbol	Ce symbols	Ce names	p-values	Common miRNAs number	Common miRNAs
LOC103694955	Atp1b4	NM_0533381	9.41E-05	8	rno-miR-15a-5p, rno-miR-15b-5p, rno-miR-16-5p, rno-miR-195-5p, rno-miR-322-5p, rno-miR-497-5p, rno-miR-503-5p, rno-miR-6326
	Atp1a2	ENSRNOT0000009329	.000165312	5	rno-miR-31a-3p, rno-miR-328a-3p, rno-miR-328b-3p, rno-miR-6326, rno-miR-874-5p
	Adcy5	ENSRNOT00000049180	6.11E-05	6	rno-miR-15a-5p, rno-miR-15b-5p, rno-miR-16-5p, rno-miR-195-5p, rno-miR-322-5p, rno-miR-497-5p
	Adrb2	ENSRNOT00000026098	.002628469	6	rno-miR-15a-5p, rno-miR-15b-5p, rno-miR-16-5p, rno-miR-195-5p, rno-miR-322-5p, rno-miR-497-5p
	Gucy1b2	ENSRNOT00000081912	.00192783	6	rno-miR-15a-5p, rno-miR-15b-5p, rno-miR-16-5p, rno-miR-195-5p, rno-miR-322-5p, rno-miR-497-5p
	Itpr1	ENSRNOT00000041130	6.55E-06	8	rno-miR-15a-5p, rno-miR-15b-5p, rno-miR-16-5p, rno-miR-195-5p, rno-miR-322-5p, rno-miR-497-5p, rno-miR-542-3p, rno-miR-6326
	Plcb4	ENSRNOT00000042853	.025446	4	rno-miR-15a-5p, rno-miR-15b-5p, rno-miR-322-5p, rno-miR-503-5p
	Prkca	ENSRNOT00000055073	.000261	6	rno-miR-15a-5p, rno-miR-15b-5p, rno-miR-16-5p, rno-miR-195-5p, rno-miR-322-5p, rno-miR-874-5p
	Slc12a2	ENSRNOT00000021921	.000183	7	rno-miR-15a-5p, rno-miR-15b-5p, rno-miR-16-5p, rno-miR-195-5p, rno-miR-322-5p, rno-miR-497-5p, rno-miR-503-5p
LOC103691854	Cd38	ENSRNOT00000004121	.000219	6	rno-miR-138-1-3p, rno-miR-182, rno-miR-29a-3p, rno-miR-29b-3p, rno-miR-29c-3p, rno-miR-770-5p
LOC102557384	Atp2b3	ENSRNOT00000077979	.000918	3	rno-miR-204-3p, rno-miR-330-5p, rno-miR-466b-5p
	Itpr2	NM_133288	.000918	4	rno-miR-103-3p, rno-miR-107-3p, rno-miR-204-3p, rno-miR-326-3p
	Nos1	ENSRNOT00000066810	.0057	3	rno-miR-202-3p, rno-miR-326-3p, rno-miR-330-5p
	Kcnma1	ENSRNOT00000077671	.018018	3	rno-miR-103-3p, rno-miR-107-3p, rno-miR-204-3p
Fancm	Tjp3	ENSRNOT00000089004	.000223	5	rno-miR-328a-3p, rno-miR-328b-3p, rno-miR-3585-3p, rno-miR-540-3p, rno-miR-92a-2-5p

(Continues)

TABLE 4 (Continued)

Gene symbol	Ce symbols	Ce names	p-values	Common miRNAs number	Common miRNAs
LOC102546383	Cd38	ENSRNOT00000004121	.002678	4	rno-miR-29a-3p, rno-miR-29b-3p, rno-miR-29c-3p, rno-miR-99a-3p
	Adcy6	ENSRNOT000000082699	.012126	4	rno-miR-204-5p, rno-miR-211-5p, rno-miR-3580-3p, rno-miR-6332
		ENSRNOT000000088323	.012126		
	Itpr3	ENSRNOT000000090925	.102875	3	rno-miR-149-3p, rno-miR-3557-3p, rno-miR-92b-5p
		NM_013138	.014853		
AC094236.1	Prkcb	NM_012713	6.63E-05	5	rno-miR-34a-5p, rno-miR-34b-5p, rno-miR-34c-5p, rno-miR-449a-5p, rno-miR-449c-5p
	Vamp2	ENSRNOT000000057295	6.06E-06	6	rno-miR-34a-5p, rno-miR-34b-5p, rno-miR-34c-5p, rno-miR-449a-5p, rno-miR-449c-5p, rno-miR-883-5p
AABR07053881.1	Cd38	ENSRNOT00000004121	.00294	3	rno-miR-122-5p, rno-miR-34a-3p, rno-miR-99a-3p

cell membrane to the cytoplasm in SMG-C6 cells (Xu et al., 2015). However, it is still unclear whether lncRNAs affect salivary secretion by regulating the expression and distribution of Aqp5. Based on our previous study, BTXA may affect the secretion of the submandibular gland by affecting the expression of Fancm, LOC10254638, and AC094236.1 to downregulate the expression and induce the redistribution of Aqp5.

Besides, Trpv6 is the Ca²⁺-selective channel of the TRP superfamily, showing expression in the salivary glands, the intestine, the kidney, and a few other tissues (Peng, Suzuki, Gyimesi, & Hediger, 2018). In human salivary glands, this molecule is expressed mainly in the basolateral membrane, suggesting a crucial role for calcium influx into acinar cells (Homann, Kinne-Saffran, Arnold, Gaengler, & Kinne, 2006). The increase in Ca²⁺ in the cytoplasm regulates a variety of ion transporters, such as Ca²⁺-activated K⁺ channel, Na⁺/K⁺/2Cl⁻ cotransporter in the basolateral membrane, and the Ca²⁺-activated Cl⁻ channel in the luminal membrane, which are closely related to fluid secretion (Ambudkar, 2016). Therefore, BTXA may decrease the influx of Ca²⁺ into acinar cells by affecting the expression of Fancm and then reducing the expression of Trpv6, thereby affecting the activity of a variety of Ca²⁺-activated ion transporters, and ultimately inhibiting salivary secretion. This study provides new insights for further exploration of BTXA-mediated inhibition of salivary secretion.

Next, we constructed a ceRNA network. We used the DAVID 6.8 database to analyze the functions of mRNAs involved in the construction of ceRNA network and found that seven lncRNAs target genes were involved in the process of salivary secretion, of which LOC103694955 had the largest number of target genes, a total of nine (shown in Table 4), including adrenoceptor beta 2 (Adrb2). As an adrenoceptor, Adrb2 is closely associated with salivary secretion. A study found that the activation of β -adrenoceptors (β -ARs) plays an important role in the regulation of cell growth and secretion of submandibular gland (Horie et al., 1996). Adrenergic fibers release norepinephrine to activate β -ARs to mediate protein secretion in the salivary glands (Baum, 1993). Lack of norepinephrine and inhibition of β -AR expression leads to insufficient secretion in the early stage of rabbit submandibular transplantation, while isoproterenol increases fluid secretion and amylase expression by upregulating β -ARs (Baum, 1993). The increase in the expression of β -ARs may lead to changes in protein secretion by promoting the interaction of syntaxin-4 and vesicle-associated membrane protein 2 in transplanted human submandibular gland (Ding et al., 2018). Through the construction of the ceRNA network, we found that the following miRNAs had binding sites on LOC103694955 and Adrb2: rno-miR-15a-5p, rno-miR-15b-5p, rno-miR-16-5p, rno-miR-195-5p, rno-miR-322-5p, and rno-miR-497-5p. A recent report suggests that miR-16-5p is highly expressed in the tears of patients with Sjögren's syndrome (Kim et al., 2019). The role of these miRNAs in the regulation of salivary gland function, however, remains unclear. Whether they play a role in BTXA-inhibited submandibular gland secretion needs further studies.

In this study, we used microarray and bioinformatic analyses to identify the changes in lncRNA and mRNA expression profiles, and

signaling pathways following BTXA injection into the submandibular gland of rats, and constructed lncRNA-mRNA co-expression and ceRNA networks to explore the regulatory relationship between the coding and non-coding genes. Our study provides the foundation for further exploring the mechanism through which BTXA inhibits salivary secretion, and provides theoretical framework for more effective clinical management of sialorrhea.

CONFLICT OF INTEREST

The authors declare that they have no conflict of interest.

AUTHOR CONTRIBUTIONS

Qian-Ying Mao: Conceptualization; Data curation; Formal analysis; Investigation; Methodology; Validation; Visualization; Writing-original draft. **ShangXie:** Data curation; Formal analysis; Investigation; Validation; Writing-review & editing. **Li-Ling Wu:** Investigation; Project administration; Resources; Supervision; Writing-review & editing. **Ruolan Xiang:** Conceptualization; Funding acquisition; Investigation; Methodology; Project administration; Resources; Writing-review & editing. **Zhigang Cai:** Conceptualization; Funding acquisition; Investigation; Methodology; Project administration; Resources; Writing-review & editing.

PEER REVIEW

The peer review history for this article is available at <https://publons.com/publon/10.1111/odi.13633>.

DATA AVAILABILITY STATEMENT

The sequencing data of this study have been deposited at the National Center for Biotechnology Information Gene Expression Omnibus (NCBI, GEO, <http://www.ncbi.nlm.gov/geo/>) under accession number GSE144985.

ORCID

Ruo-Lan Xiang  <https://orcid.org/0000-0001-5935-1911>

REFERENCES

- Ambudkar, I. S. (2016). Calcium signalling in salivary gland physiology and dysfunction. *Journal of Physiology*, *594*, 2813–2824. <https://doi.org/10.1113/jp271143>
- Baum, B. J. (1993). Principles of saliva secretion. *Annals of the New York Academy of Sciences*, *694*, 17–23. <https://doi.org/10.1111/j.1749-6632.1993.tb18338.x>
- Chen, Z., Lin, S., Li, J.-L., Ni, W., Guo, R., Lu, J., ... Wu, L. (2018). CRTC1-MAML2 fusion-induced lncRNA LINC00473 expression maintains the growth and survival of human mucoepidermoid carcinoma cells. *Oncogene*, *37*, 1885–1895. <https://doi.org/10.1038/s4138-017-0104-0>
- Delporte, C. (2014). Aquaporins in salivary glands and pancreas. *Biochimica Et Biophysica Acta*, *1840*, 1524–1532. <https://doi.org/10.1016/j.bbagen.2013.08.007>
- Ding, C., Cong, X., Zhang, Y., Li, S. L., Wu, L. L., & Yu, G. Y. (2018). beta-adrenoceptor activation increased VAMP-2 and syntaxin-4 in secretory granules are involved in protein secretion of submandibular gland through the PKA/F-actin pathway. *Bioscience Reports*, *38*, BSR20171142. <https://doi.org/10.1042/BSR20171142>
- Evans, R. L., Park, K., Turner, R. J., Watson, G. E., Nguyen, H. V., Dennett, M. R., ... Melvin, J. E. (2000). Severe impairment of salivation in Na⁺/K⁺/2Cl⁻ cotransporter (NKCC1)-deficient mice. *Journal of Biological Chemistry*, *275*, 26720–26726. <https://doi.org/10.1074/jbc.M003753200>
- Homann, V., Kinne-Saffran, E., Arnold, W. H., Gaengler, P., & Kinne, R. K. (2006). Calcium transport in human salivary glands: A proposed model of calcium secretion into saliva. *Histochemistry and Cell Biology*, *125*, 583–591. <https://doi.org/10.1007/s00418-005-0100-2>
- Horie, K., Kagami, H., Hiramatsu, Y., Hata, K., Shigetomi, T., & Ueda, M. (1996). Selected salivary-gland cell culture and the effects of isoproterenol, vasoactive intestinal polypeptide and substance P. *Archives of Oral Biology*, *41*, 243–252. [https://doi.org/10.1016/0003-9969\(95\)00132-8](https://doi.org/10.1016/0003-9969(95)00132-8)
- Inoue, N., Iida, H., Yuan, Z., Ishikawa, Y., & Ishida, H. (2003). Age-related decreases in the response of aquaporin-5 to acetylcholine in rat parotid glands. *Journal of Dental Research*, *82*, 476–480. <https://doi.org/10.1177/154405910308200614>
- Kawedia, J. D., Nieman, M. L., Boivin, G. P., Melvin, J. E., Kikuchi, K.-I., Hand, A. R., ... Menon, A. G. (2007). Interaction between transcellular and paracellular water transport pathways through Aquaporin 5 and the tight junction complex. *Proceedings of the National Academy of Sciences USA*, *104*, 3621–3626. <https://doi.org/10.1073/pnas.0608384104>
- Kim, Y. J., Yeon, Y., Lee, W. J., Shin, Y. U., Cho, H., Sung, Y. K., ... Kang, M. H. (2019). Comparison of MicroRNA expression in tears of normal subjects and Sjogren syndrome patients. *Investigative Ophthalmology & Visual Science*, *60*, 4889–4895. <https://doi.org/10.1167/iovs.19-27062>
- Krane, C. M., Melvin, J. E., Nguyen, H. V., Richardson, L., Towne, J. E., Doetschman, T., & Menon, A. G. (2001). Salivary acinar cells from aquaporin 5-deficient mice have decreased membrane water permeability and altered cell volume regulation. *Journal of Biological Chemistry*, *276*, 23413–23420. <https://doi.org/10.1074/jbc.M008760200>
- Miao, Y. Y., Liu, J., Zhu, J., Tao, Y. L., Zhang, J. A., Luo, D., & Zhou, B. R. (2017). The effect of botulinum toxin type A on expression profiling of long noncoding RNAs in human dermal fibroblasts. *BioMed Research International*, *2017*, 2957941. <https://doi.org/10.1155/2017/2957941>
- Mukaibo, T., Munemasa, T., George, A. T., Tran, D. T., Gao, X., Herche, J. L., ... Melvin, J. E. (2018). The apical anion exchanger Slc26a6 promotes oxalate secretion by murine submandibular gland acinar cells. *Journal of Biological Chemistry*, *293*, 6259–6268. <https://doi.org/10.1074/jbc.RA118.002378>
- Naumann, M., & Jost, W. (2004). Botulinum toxin treatment of secretory disorders. *Movement Disorders*, *19*(Suppl. 8), S137–S141. <https://doi.org/10.1002/mds.20067>
- Ohana, E. (2015). Transepithelial ion transport across duct cells of the salivary gland. *Oral Diseases*, *21*, 826–835. <https://doi.org/10.1111/odi.12201>
- Ohana, E., Yang, D., Shcheynikov, N., & Muallem, S. (2009). Diverse transport modes by the solute carrier 26 family of anion transporters. *Journal of Physiology*, *587*, 2179–2185. <https://doi.org/10.1113/jphysiol.2008.164863>
- Peng, J. B., Suzuki, Y., Gyimesi, G., & Hediger, M. A. (2018). TRPV5 and TRPV6 calcium-selective channels. In J. A. Kozak, & J. W. Putney Jr. (Eds.), *Calcium entry channels in non-excitabile cells* (pp. 241–274). Boca Raton, FL: CRC Press/Taylor & Francis.
- Romanenko, V., Nakamoto, T., Srivastava, A., Melvin, J. E., & Begenisich, T. (2006). Molecular identification and physiological roles of parotid acinar cell maxi-K channels. *Journal of Biological Chemistry*, *281*, 27964–27972. <https://doi.org/10.1074/jbc.M603871200>
- Shan, X. F., Xu, H., Cai, Z. G., Wu, L. L., & Yu, G. Y. (2013). Botulinum toxin A inhibits salivary secretion of rabbit submandibular gland.

- International Journal of Oral Science*, 5, 217–223. <https://doi.org/10.1038/ijos.2013.82>
- Shi, H., Cao, N., Pu, Y., Xie, L., Zheng, L., & Yu, C. (2016). Long non-coding RNA expression profile in minor salivary gland of primary Sjogren's syndrome. *Arthritis Research & Therapy*, 18, 109. <https://doi.org/10.1186/s13075-016-1005-2>
- Srivanitchapoom, P., Pandey, S., & Hallett, M. (2014). Drooling in Parkinson's disease: A review. *Parkinsonism & Related Disorders*, 20, 1109–1118. <https://doi.org/10.1016/j.parkreldis.2014.08.013>
- Steinfeld, S., Cogan, E., King, L. S., Agre, P., Kiss, R., & Delporte, C. (2001). Abnormal distribution of aquaporin-5 water channel protein in salivary glands from Sjogren's syndrome patients. *Laboratory Investigation*, 81, 143–148. <https://doi.org/10.1038/labinvest.3780221>
- Vashishta, R., Nguyen, S. A., White, D. R., & Gillespie, M. B. (2013). Botulinum toxin for the treatment of sialorrhea: A meta-analysis. *Otolaryngology - Head and Neck Surgery*, 148, 191–196. <https://doi.org/10.1177/0194599812465059>
- Walshe, M., Smith, M., & Pennington, L. (2012). Interventions for drooling in children with cerebral palsy. *Cochrane Database Systematic Review*, 11, CD008624. <https://doi.org/10.1002/14651858.CD008624.pub3>
- Wheeler, A., & Smith, H. S. (2013). Botulinum toxins: Mechanisms of action, antinociception and clinical applications. *Toxicology*, 306, 124–146. <https://doi.org/10.1016/j.tox.2013.02.006>
- Xie, S., Xu, H., Shan, X. F., & Cai, Z. G. (2019). Botulinum toxin type A interrupts autophagic flux of submandibular gland. *Bioscience Reports*, 39, BSR20190035. <https://doi.org/10.1042/BSR20190035>
- Xie, S., Yu, X., Li, Y., Ma, H., Fan, S., Chen, W., ... Lin, Z. (2018). Upregulation of lncRNA ADAMTS9-AS2 promotes salivary adenoid cystic carcinoma metastasis via PI3K/Akt and MEK/Erk signaling. *Molecular Therapy*, 26, 2766–2778. <https://doi.org/10.1016/j.ymthe.2018.08.018>
- Xu, H., Shan, X. F., Cong, X., Yang, N. Y., Wu, L. L., Yu, G. Y., ... Cai, Z. G. (2015). Pre- and post-synaptic effects of botulinum toxin A on submandibular glands. *Journal of Dental Research*, 94, 1454–1462. <https://doi.org/10.1177/0022034515590087>
- Xu, W., Liu, L., Lu, H., Fu, J., Zhang, C., Yang, W., & Shen, S. (2019). Dysregulated long noncoding RNAs in pleomorphic adenoma tissues of pleomorphic adenoma gene 1 transgenic mice. *Molecular Medicine Reports*, 19, 4735–4742. <https://doi.org/10.3892/mmr.2019.10149>

SUPPORTING INFORMATION

Additional supporting information may be found online in the Supporting Information section.

How to cite this article: Mao Q-Y, Xie S, Wu L-L, Xiang R-L, Cai Z-G. Aberrantly expressed lncRNAs and mRNAs after botulinum toxin type A inhibiting salivary secretion. *Oral Dis*. 2021;27:1171–1183. <https://doi.org/10.1111/odi.13633>